Formation and Characterization of Two FeO_3 Isomers in Solid Argon

Yu Gong and Mingfei Zhou*

Department of Chemistry, Shanghai Key Laboratory of Molecular Catalysts and Innovative Materials, Advanced Materials Laboratory, Fudan University, Shanghai 200433, P. R. China

Received: July 22, 2008; Revised Manuscript Received: September 4, 2008

Two FeO_3 isomers were prepared and characterized using matrix isolation infrared spectroscopy and theoretical calculations. The iron monoxide molecules produced from laser evaporation of the bulk iron oxide target react with dioxygen in solid argon to form the $(\eta^2\text{-}O_2)FeO$ complex spontaneously on annealing. The $(\eta^2\text{-}O_2)FeO$ complex was predicted to have a $^5B_2$ ground state with a planar C_{2v} structure, in which the O_2 fragment is side-on bonded to the iron center. The $(\eta^2\text{-}O_2)FeO$ complex rearranges to the more stable iron trioxide isomer upon visible light ($\lambda > 500$ nm) irradiation. The iron trioxide molecule was predicted to have a closed-shell singlet ground state with a planar D_{3h} symmetry, in which the iron possesses a +6 oxidation state.

Introduction

Oxidation of iron is an important subject in material corrosion and biochemical process. Great efforts were made on the preparation and characterization of iron oxides and dioxygen complexes. The electronic and geometric structures of simple iron oxides have been the subject of various experimental and theoretical studies. As the first member in the FeO_x series, iron monoxide has been well studied both in the gas phase and in solid noble gas matrixes.[1−11] The FeO_2 molecules in the form of oxo, peroxo, and superoxo were proposed to be reaction products between the iron atom and molecular oxygen in solid matrixes.[12−16] However, gas phase investigations indicate that ground-state iron atoms are unreactive toward dioxygen at room temperature.[17,18] Anion photoelectron spectroscopic investigation also indicates that only the inserted OFeO structure was observed.[5,19] A recent matrix isolation infrared spectroscopic study in this laboratory shows that iron atoms react with dioxygen to form the inserted FeO_2 molecule only under UV−visible light excitation and that the cyclic $Fe(O_2)$ and FeOO species are not able to be formed.[20] As for the FeO_4 species, pure DFT calculations found that a tetraoxide structure (T_d symmetry) without O−O bonding is more stable than the $(\eta^2\text{-}O_2)FeO_2$ structure, which was predicted to have a singlet ground state with a nonplanar C_{2v} symmetry.[21,22] However, ab initio and hybrid DFT calculations revealed that the tetraoxide structure is less stable than the $(\eta^2\text{-}O_2)FeO_2$ structure.[23] Anion photoelectron spectroscopic study also suggested that the observed FeO_4 species is due to $(\eta^2\text{-}O_2)FeO_2$.[19] Both the side-on and end-on bonded dioxygen−iron dioxide complexes were formed via the reactions between FeO_2 and O_2 in solid argon. These two isomers are interconvertible under different wavelength range photoexcitation.[20]

The FeO_3 species has also been the subject of some experimental and theoretical investigations. In an anion photoelectron spectroscopic investigation, the FeO_3 species observed in the gas phase was proposed to possess a D_{3h} symmetry with all the oxygen atoms atomically bound to the iron center.[19] In the photo-oxidation of matrix isolated iron pentacarbonyl in the presence of oxygen, a 945 cm^{-1} absorption was attributed to the doubly degenerate Fe═O stretch vibration of iron trioxide.[14] However, this absorption was reassigned to the inserted OFeO molecule in a late investigation on the reactions of laser ablated iron atoms with dioxygen.[15] Instead, a 975.8 cm^{-1} absorption was tentatively assigned to the trioxide molecule in that report. In this paper, we provide a joint matrix isolation infrared spectroscopic and theoretical investigation on the formation and characterization of two FeO_3 isomers, which were formed via the reactions of laser-evaporated iron monoxide and O_2 in solid argon.

Experimental and Computational Methods

The experimental setup for pulsed laser evaporation and matrix isolation infrared spectroscopic investigation has been described in detail previously.[24] Briefly, the 1064 nm fundamental of a Nd:YAG laser (Continuum, Minilite II, 10 Hz repetition rate, and 6 ns pulse width) was focused onto a rotating iron oxide or metallic iron target through a hole in a CsI window cooled normally to 6 K by means of a closed-cycle helium refrigerator (ARS, 202N). The laser-evaporated metal atoms were codeposited with oxygen/argon mixtures onto the CsI window. In general, matrix samples were deposited for 1 h at a rate of approximately 4 mmol/h. The O_2/Ar mixtures were prepared in a stainless steel vacuum line using a standard manometric technique. Isotopic $^{18}O_2$ (ISOTEC, 99%) was used without further purification. The infrared absorption spectra of the resulting samples were recorded on a Bruker IFS 66V spectrometer at 0.5 cm^{-1} resolution between 4000 and 450 cm^{-1} using a liquid nitrogen cooled HgCdTe (MCT) detector. Samples were annealed to different temperatures and cooled back to 6 K for spectral acquisition. Selected samples were subjected to broadband irradiation using a tungsten lamp with a $\lambda > 500$ nm long wavelength pass glass filter.

Quantum chemical calculations were performed using the Gaussian 03 program.[25] The nonlocal exchange functional according to Becke with additional correlation corrections due to Perdew (BP86) was utilized.[26,27] According to our theoretical investigations, this method was the best one to reproduce the experimental frequencies and isotopic ratios on the FeO_3 system. The 6-311+G(d) basis set was used for the O atom, and the all electron basis set of Wachters−Hay as modified by Gaussian was used for the Fe atom.[28] The geometries were fully optimized; the harmonic vibrational frequencies were calculated; and zero-point vibrational energies (ZPVE) were derived.

* Corresponding author. E-mail: mfzhou@fudan.edu.cn.

10.1021/jp806442y CCC: $40.75
Published on Web 10/02/2008

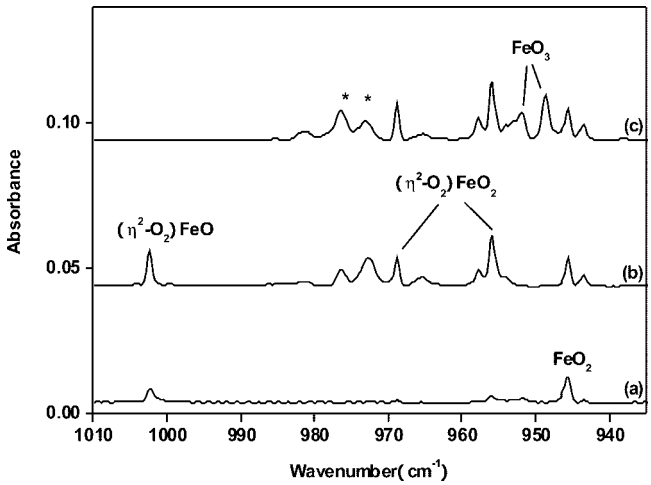

Figure 1. Infrared spectra in the 1010−935 cm^{-1} region from codeposition of laser-evaporated iron oxide with 0.5% O_2 in argon. (a) 1 h of sample deposition at 6 K, (b) after 25 K annealing, and (c) after 15 min of $\lambda > 500$ nm irradiation. (The absorptions labeled with an asterisk are due to Fe_xO_y clusters.)

Results and Discussions

Infrared Spectra. The FeO_3 species were formed via the reaction of iron monoxide with dioxygen in solid argon. Laser evaporation of an Fe_2O_3 target under controlled laser energy (approximately 2 mJ/pulse) followed by co-condensation with pure argon at 6 K revealed a strong absorption at 873.1 cm^{-1}. This absorption was previously assigned to FeO,[15] but recent investigation in this group indicates that it should be regarded as an argon atom coordinated ArFeO complex instead of the isolated diatomic molecule.[29] The gas phase fundamental of FeO was determined to be 871.3 cm^{-1} from electronic spectra,[3] suggesting that the matrix shift is rather small. When the laser-evaporated iron oxide species were codeposited with the O_2/Ar mixture, new product absorptions were observed. The infrared spectra in the 1010−935 cm^{-1} region with 0.5% O_2 in argon are shown in Figure 1, and the product absorptions are listed in Table 1. After one hour of sample deposition, weak absorptions at 945.8 and 797.1 cm^{-1} which were previously assigned to the antisymmetric and symmetric stretching modes of the inserted FeO_2 molecule were also observed along with the strong ArFeO absorption (not shown).[15] When the sample was annealed to 25 K (Figure 1, trace b), the FeO_2 absorptions decreased with the formation of the end-on and side-on bonded iron dioxide−dioxygen complexes.[20] Since the end-on bonded complex spontaneously rearranged to the side-on bonded complex when the sample was irradiated by the light emitted from the IR source, the end-on bonded (η^1-OO)FeO_2 complex absorptions were barely observed if the sample was scanned over 100 times. Besides the above-mentioned absorptions, a new absorption at 1002.3 cm^{-1} was also observed, which increased markedly upon sample annealing at the expense of the ArFeO absorption. The 1002.3 cm^{-1} absorption is photosensitive. It was completely destroyed upon visible light irradiation ($\lambda > 500$ nm), during which two absorptions at 948.6 and 951.9 cm^{-1} were produced (Figure 1, trace c). Experiments were repeated using an isotopic substituted $^{18}O_2$ sample and the $^{16}O_2 + {}^{18}O_2$ and $^{16}O_2 + {}^{16}O^{18}O + {}^{18}O_2$ mixtures. The difference spectra (spectrum taken after 25 K annealing followed by 15 min of $\lambda > 500$ nm irradiation minus spectrum taken right after 25 K annealing) in selected regions from codeposition of laser-evaporated iron oxides with different isotopic samples are shown in Figure 2.

The experiments on the reaction of laser-evaporated iron atoms and dioxygen in excess argon were also performed. In the reaction of iron and $^{16}O_2$, the inserted FeO_2 absorptions dominate the spectrum. The ArFeO absorption is much weaker than that in the experiment with the bulk Fe_2O_3 target. The 1002.3, 948.6, and 951.9 cm^{-1} absorptions were produced upon sample annealing or visible light irradiation, but their IR intensities are very low as well. To get the band positions of all oxygen-18 substituted products, a similar experiment on the reaction of the iron atom and $^{18}O_2$ was performed; the 1002.3, 948.6, and 951.9 cm^{-1} absorptions were shifted; and the isotopic frequencies are also listed in Table 1.

(η^2-O_2)FeO. In the experiment with a bulk iron oxide target, the 1002.3 cm^{-1} absorption shifted to 959.2 cm^{-1} when an $^{18}O_2$/Ar sample was used. The spectra from similar experiments using $^{16}O_2 + {}^{18}O_2$ and $^{16}O_2 + {}^{16}O^{18}O + {}^{18}O_2$ mixtures with a bulk iron oxide target revealed that one O_2 fragment with two equivalent O atoms is involved in this mode (Figure 2, traces c and d) and that the O_2 fragment comes from the O_2 reagent. The 1002.3 cm^{-1} absorption was also observed in the iron atom and O_2 reaction, which shifted to 952.0 cm^{-1} when the $^{18}O_2$/Ar sample was used. The 952.0 cm^{-1} absorption should be due to the all oxygen-18 substituted product. The absorption observed at 959.2 cm^{-1} in the reaction of iron oxide species from the bulk oxide target and $^{18}O_2$ is about 7.2 cm^{-1} blue-shifted from the all oxygen-18 substituted value of 952.0 cm^{-1}. This observation suggests that the 1002.3 cm^{-1} absorber involves an additional oxygen atom from laser evaporation of the bulk iron oxide target. The experimental observations indicate that the intensity of the 1002.3 cm^{-1} absorption depends strongly on the ArFeO absorption, which suggests that the absorber should be due to a reaction product between ArFeO and dioxygen. Therefore, we assign the 1002.3 cm^{-1} absorption to a (η^2-O_2)FeO complex. The $^{16}O/^{18}O$ isotopic frequency ratio (1.0528) indicates that the 1002.3 cm^{-1} absorption is not due to a pure O−O stretch mode but is strongly coupled with the Fe═O stretch mode (referred as O−O stretch mode hereafter). The 959.2 cm^{-1} absorption is due to the partially oxygen-18 substituted (η^2-$^{18}O_2$)FeO isotopomer, while the 952.0 cm^{-1} absorption is attributed to the all oxygen-18 substituted (η^2-$^{18}O_2$)$Fe^{18}O$ molecule.

To support the experimental assignment, quantum chemical calculations were carried out on the (η^2-O_2)FeO complex. At the DFT/BP86 level of theory, the (η^2-O_2)FeO complex was predicted to have a $^5B_2$ ground state with a planar C_{2v} geometry (Figure 3). The Fe═O distance was calculated to be 1.619 Å, close to the values of previously characterized FeO containing species.[30,31] The O−O bond length was predicted to be 1.369 Å. Frequency calculations show that the experimentally observed mode is located at 1035.3 cm^{-1}, about 30 cm^{-1} higher than the observed value (Table 2). The calculated isotopic frequency ratio also fits the observed value (Table 3). Different from a number of recently characterized transition-metal dioxygen complexes,[20,32] the predicted bond length of the (η^2-O_2)FeO complex lies on the boundary between the typical superoxo anion and peroxo dianion.[33] Hence, it is more reasonable to consider the (η^2-O_2)FeO complex as an intermediate between superoxide and peroxide. Consistent with this notion, spin density on the O_2 moiety was calculated to be 0.51, a value intermediate between an ideal superoxo anion (1.0) and a peroxo dianion (0.0). The (η^2-O_2)FeO complex is expected to have seven vibrational modes. As can be seen in Table 2, the O−O stretch mode has the largest IR intensity, and all of the other vibrational modes were predicted to have much lower IR intensities than that of

TABLE 1: Infrared Absorptions (cm^{-1}) from Codeposition of Laser-Evaporated FeO with O_2 in Solid Argon

$^{16}O_2$	$^{18}O_2$	$^{16}O_2 + {}^{18}O_2$	$^{16}O_2 + {}^{16}O^{18}O + {}^{18}O_2$	$^{18}O_2$[a]	assignment
1002.3	959.2	1002.3, 959.2	1002.3, 980.4, 959.2	952.0	(η^2-O_2)FeO, O−O str.
951.9	942.5, 915.4	951.9, 942.5, 915.4	951.9, 942.5, 915.4	915.1	FeO_3, Fe═O str. site
948.6	938.4, 913.1	948.6, 938.4, 913.1	948.6, 938.4, 913.1	912.4	FeO_3, Fe═O str.

[a] Absorptions observed in the reaction of Fe and $^{18}O_2$.

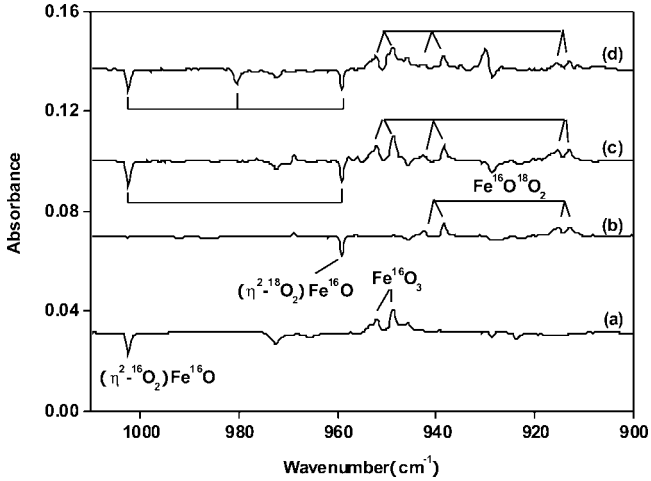

Figure 2. Difference spectra in the 1010−900 cm^{-1} region with different isotopic samples. (a) 0.5% $^{16}O_2$, (b) 0.5% $^{18}O_2$, (c) 0.25% $^{16}O_2$ + 0.25% $^{18}O_2$, and (d) 0.15% $^{16}O_2$ + 0.3% $^{16}O^{18}O$ + 0.15% $^{18}O_2$ (spectrum taken after 25 K annealing followed by 15 min of $\lambda > 500$ nm irradiation minus spectrum taken right after 25 K annealing).

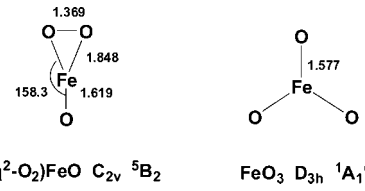

Figure 3. Optimized structures (bond lengths in angstrom and bond angles in degree) of the observed FeO_3 isomers.

TABLE 2: DFT/BP86 Calculated Total Energies[a], Vibrational Frequencies (cm^{-1}), and Intensities (km/mol) of the Two FeO_3 Isomers

molecule	energy	frequency (intensity)
(η^2-O_2)FeO ($^5B_2$, C_{2v})	−1489.540097	1035.3 (176), 929.5 (15), 595.9 (2), 495.9 (0), 156.2 (24), 55.1(15)
FeO_3 ($^1A_1'$, D_{3h})	−1489.593365	1021.3 (105 × 2), 917.6 (0), 331.4 (0 × 2), 150.9 (12)

[a] In Hartree, after zero-point energy corrections.

the O−O vibration. Therefore, only the O−O stretch mode is experimentally observed.

In the previous experiments on the reaction of laser-ablated iron with dioxygen in solid argon,[15] the 1002.3 cm^{-1} absorption together with a 2271.3 cm^{-1} absorption was tentatively assigned to the Fe═O and N−N stretch modes of a N_2FeO_2 complex, while two absorptions at 1147.5 and 928.1 cm^{-1} were tentatively assigned to the O−O and Fe═O stretch vibrations of the (η^2-O_2)FeO complex. In the present experiments, no absorptions were observed around 2271 cm^{-1} that tracks with the 1002.3 cm^{-1} absorption. The spectra around the 1150 cm^{-1} region are very clean, and no absorption that correlates to the previously reported 1147.5 cm^{-1} absorption was observed. In addition, the present theoretical calculations can rule out the possibility for assigning the 1147.5 and 928.1 cm^{-1} absorptions to the (η^2-O_2)FeO complex.

TABLE 3: Comparison between the Observed and Calculated Vibrational Frequencies (cm^{-1}) and Isotopic Frequency Ratios of the Two FeO_3 Isomers

		freq		$^{16}O/^{18}O$[a]	
molecule	mode	calcd	obsd	calcd	obsd
(η^2-O_2)FeO ($^5B_2$, C_{2v})	O−O str. (a_1)	1035.3	1002.3	1.0555	1.0528
FeO_3 ($^1A_1'$, D_{3h})	Fe═O str. (e′)	1021.3	948.6	1.0403	1.0397

[a] Oxygen-18 refers to $Fe^{18}O_3$.

FeO_3. The 948.6 and 951.9 cm^{-1} absorptions were produced only under visible light irradiation, during which the (η^2-O_2)FeO complex absorption was destroyed. This suggests that the absorber of the 948.6 and 951.9 cm^{-1} absorptions should be due to a structural isomer of (η^2-O_2)FeO. The experiment using a metallic iron target and $^{18}O_2$ revealed that the 948.6/951.9 cm^{-1} absorptions shifted to 912.4 and 915.1 cm^{-1}. Both absorptions exhibited an isotopic $^{16}O/^{18}O$ ratio of 1.0403 that is characteristic of a Fe═O stretch vibration. In the spectrum with a bulk iron oxide target and $^{18}O_2$ (Figure 2, trace b), the 948.6/951.9 cm^{-1} absorptions split into two doublets at 938.4/942.5 and 913.1/915.4 cm^{-1}. These two doublets together with the 948.6/951.9 cm^{-1} doublet were also observed in the spectra when the $^{16}O_2 + {}^{18}O_2$ and $^{16}O_2 + {}^{16}O^{18}O + {}^{18}O_2$ mixed samples were used. These spectral features indicate that the observed Fe═O stretch vibration is due to a doubly degenerate mode involving three equivalent oxygen atoms. Therefore, the 948.6 and 951.9 cm^{-1} absorptions are assigned to the doubly degenerate Fe═O stretch mode of the iron trioxide molecule. The intensities for the 948.6 and 951.9 cm^{-1} absorptions are quite different; therefore, these two absorptions are assigned to different trapping sites rather than to the degenerate mode split by the crystal field. The observation of only one Fe═O stretch mode suggests that the FeO_3 molecule is planar with a D_{3h} symmetry. In the previous experiments on the reaction of a laser-ablated iron atom with dioxygen in solid argon,[15] an absorption at 975.8 cm^{-1} was tentatively assigned to the Fe═O stretch vibrational mode of iron trioxide. This absorption was recently reassigned to the antisymmetric FeO_2 stretch vibrational mode of the (η^1-O_2)FeO_2 complex.[20]

The assignment of FeO_3 is strongly supported by DFT/BP86 calculations. As shown in Figure 3, the iron trioxide molecule was computed to have a closed-shell singlet ground state with a planar D_{3h} symmetry, in agreement with the previous DFT studies.[15,16,21,34] The lowest triplet state was predicted to be 9.1 kcal/mol higher in energy than the singlet state. The three equivalent Fe═O bond length was predicted to be 1.577 Å, slightly shorter than the value of the (η^2-O_2)FeO complex. The doubly degenerate Fe═O stretch mode was calculated at 1021.3 cm^{-1}. On the basis of theoretical calculations, this mode is the only vibration that has appreciable IR intensity which can be observed above 400 cm^{-1} (Table 2). This mode splits into a doublet when two of the oxygen atoms are substituted by O-18

due to the reduction of symmetry. Accordingly, the absorptions at 938.4/942.5 and 913.1/915.4 cm^{-1} observed in the reaction of $Fe^{16}O$ and $^{18}O_2$ are assigned to the C_{2v} $Fe^{18}O_2{}^{16}O$ isotopomer formed from the isomerization of the (η^2-$^{18}O_2$)$Fe^{16}O$ complex. The nondegenerate symmetric Fe═O stretch mode of the planar D_{3h} FeO_3 molecule is IR inactive, and this mode was predicted at 917.6 cm^{-1}. A previous photoelectron spectroscopic study in the gas phase yielded the symmetric Fe═O stretch vibrational frequency for FeO_3 to be 850 ± 50 cm^{-1}.[19]

Some transition metal trioxide species have been trapped and identified in the solid matrix.[35,36] The Fe═O stretch vibrational frequency of FeO_3 is close to the corresponding value of OsO_3 with the same symmetry but is about 50 cm^{-1} higher than that of RuO_3.[35] This trend indicates that the relativistic contraction plays a more important role than the shell expansion for the last member of this group. A similar trend has been observed for some transition metal dioxides.[15,35−38] Note that the vibrational frequency and the predicted bond length of FeO_3 are about the same as those of CrO_3, in which the metal center also possesses a +6 oxidation state.[36] The similarities between the two molecules indicates that the two extra electrons of iron may not participate in bonding with oxygen. Consistent with this deduction, bonding analysis revealed that the two electrons are mainly localized in a nonbonding orbital, which is largely a d_z^2 orbital of the iron in character.

Reaction Mechanism. Laser evaporation of bulk iron oxide target yields iron monoxide as the major product. Therefore, a substantial amount of iron monoxide molecules are able to be trapped and isolated in solid argon, and their reactions with dioxygen were investigated. Although the FeO molecules trapped in solid argon are coordinated by one argon atom, the binding energy of the ArFeO complex is very low (predicted to be 1.7 kcal/mol), and it is reasonable to refer to ArFeO as FeO for simplicity in discussion. The spectra shown in Figure 1 clearly demonstrate that the ground state of iron monoxide reacts with dioxygen to form the (η^2-O_2)FeO complex spontaneously on annealing, reaction 1. The spontaneous reaction indicates that this association reaction requires negligible activation energy. On the basis of DFT/BP86 calculations, the formation of the (η^2-O_2)FeO complex is exothermic by 52.0 kcal/mol.

$$FeO(^5\Delta) + O_2(^3\Sigma_g^-) \rightarrow (\eta^2\text{-}O_2)FeO(^5B_2)$$
$$\Delta E = -52.0\ \text{kcal/mol} \quad (1)$$

The (η^2-O_2)FeO complex is photosensitive. It was converted to the iron trioxide isomer under visible light ($\lambda > 500$ nm) irradiation. The iron trioxide structure was predicted to be 33.4 kcal/mol more stable than the (η^2-O_2)FeO complex (reaction 2). The observation of this isomerization reaction only under visible light irradiation suggests that reaction 2 requires activation energy.

$$(\eta^2\text{-}O_2)FeO(^5B_2) \rightarrow FeO_3(^1A1')$$
$$\Delta E = -33.4\ \text{kcal/mol} \quad (2)$$

Recently, a similar (η^2-O_2)TiO complex was produced via the reaction of TiO with O_2 in solid argon.[39] The (η^2-O_2)TiO complex was characterized to be a typical peroxo complex with a highly activated O−O bond (1.471 Å calculated at the B3LYP/6-311+G* level). It was found that the oxygen atoms of the peroxo ligand in (η^2-O_2)TiO can be interconverted with the oxygen atom of the monoxide subunit during the association reaction process. The O−O bond of the (η^2-O_2)FeO complex is less activated. The predicted O−O bond length of 1.369 Å is significantly shorter than that of (η^2-O_2)TiO. As can be seen in Figure 2, no intermediate absorptions can be found for the O−O stretch vibration of (η^2-O_2)FeO when the $^{18}O_2$ and $^{16}O_2 + {}^{18}O_2$ samples were used, which indicates that the oxygen atoms of the O_2 ligand in (η^2-O_2)FeO cannot be interconverted with the oxygen atom of the monoxide subunit.

Conclusions

The reaction of iron monoxide and dioxygen was studied using matrix isolation infrared spectroscopy and theoretical calculations. The FeO molecules were produced by pulse laser evaporation of the bulk iron oxide target. The ground state of FeO molecules reacted with O_2 in solid argon to form the (η^2-O_2)FeO complex spontaneously on sample annealing. Density functional theoretical calculations indicate that the (η^2-O_2)FeO complex possessed a $^5B_2$ ground state with a planar C_{2v} symmetry. The O_2 ligand is side-on bonded which can be described as an intermediate between a peroxo dianion and a superoxo anion. The (η^2-O_2)FeO complex undergoes photoinduced isomerization to give the more stable iron trioxide isomer upon visible light irradiation. The iron trioxide molecule was predicted to have a closed-shell singlet ground state with a planar D_{3h} symmetry. The results show that the oxidation of iron monoxide was initiated from the formation of the (η^2-O_2)FeO complex and ends up with the production of iron trioxide, which was the most stable configuration along the reaction coordinate.

Acknowledgment. This work is supported by the National Basic Research Program of China (2007CB815203) and the National Natural Science Foundation of China (20433080 and 20773030).

References and Notes

(1) Green, D. W.; Reedy, G. T.; Kay, J. G. *J. Mol. Spectrosc.* **1979**, *78*, 257.
(2) (a) Andersen, T.; Lykke, K. R.; Neumark, D. M.; Lineberger, W. C. *J. Chem. Phys.* **1987**, *86*, 1858. (b) Engelking, P. C.; Lineberger, W. C. *J. Chem. Phys.* **1977**, *66*, 5054.
(3) (a) Cheung, A. S.-C.; Lee, N.; Lyyra, A. M.; Merer, A. J.; Taylor, A. W. *J. Mol. Spectrosc.* **1982**, *95*, 213. (b) Cheung, A. S.-C.; Lyyra, A. M.; Merer, A. J.; Taylor, A. W. *J. Mol. Spectrosc.* **1983**, *102*, 224. (c) Taylor, A. W.; Cheung, A. S.-C.; Merer, A. J. *J. Mol. Spectrosc.* **1985**, *113*, 487.
(4) (a) Kröckertskothen, T.; Knöckel, H.; Tiemann, E. *Chem. Phys.* **1986**, *103*, 335. (b) Kröckertskothen, T.; Knöckel, H.; Tiemann, E. *Mol. Phys.* **1987**, *62*, 1031.
(5) Fan, J.; Wang, L. S. *J. Chem. Phys.* **1995**, *102*, 8714.
(6) Son, H. S.; Lee, K.; Shin, S. K.; Ku, J. K. *Chem. Phys. Lett.* **2000**, *320*, 658.
(7) Chestakov, D. A.; Parker, D. H.; Baklanov, A. V. *J. Chem. Phys.* **2005**, *122*, 084302.
(8) Metz, R. B.; Nicolas, C.; Ahmed, M.; Leone, S. R. *J. Chem. Phys.* **2005**, *123*, 114313.
(9) (a) Gutsev, G. L.; Andrews, L.; Bauschlicher, C. W., Jr. *Theor. Chem. Acc.* **2003**, *109*, 298. (b) Gutsev, G. L.; Rao, B. K.; Jena, P. *J. Phys. Chem. A* **2000**, *104*, 5374.
(10) Krauss, M.; Stevens, W. J. *J. Chem. Phys.* **1985**, *82*, 5584.
(11) Bagus, P. S.; Preston, H. J. T. *J. Chem. Phys.* **1973**, *59*, 2986.
(12) Abramowitz, S.; Acquista, N.; Levin, I. W. *Chem. Phys. Lett.* **1977**, *50*, 423.
(13) Chang, S.; Blyholder, G.; Fernandez, J. *Inorg. Chem.* **1981**, *20*, 2813.
(14) Fanfarillo, M.; Downs, A. J.; Green, T. M.; Almond, M. J. *Inorg. Chem.* **1992**, *31*, 2973.
(15) (a) Andrews, L.; Chertihin, G. V.; Ricca, A.; Bauschlicher, C. W., Jr. *J. Am. Chem. Soc.* **1996**, *118*, 467. (b) Chertihin, G. V.; Saffel, W.; Yustein, J. T.; Andrews, L.; Neurock, M.; Ricca, A.; Bauschlicher, C. W., Jr. *J. Phys. Chem.* **1996**, *100*, 5261.
(16) Yamada, Y.; Sumino, H.; Okamura, Y.; Shimasaki, H.; Tominaga, T. *Appl. Radiat. Isot.* **2000**, *52*, 157.
(17) Whetten, R. L.; Cox, D. M.; Trevor, D. J.; Kaldor, A. *J. Phys. Chem.* **1985**, *89*, 566.
(18) Mitchell, S. A.; Hackett, P. A. *J. Chem. Phys.* **1990**, *93*, 7822.

(19) (a) Wu, H. B.; Desai, S. R.; Wang, L. S. *J. Am. Chem. Soc.* **1996**, *118*, 5296. (b) Wu, H. B.; Desai, S. R.; Wang, L. S. *J. Am. Chem. Soc.* **1996**, *118*, 7434.

(20) Gong, Y.; Zhou, M. F.; Andrews, L. *J. Phys. Chem. A* **2007**, *111*, 12001.

(21) (a) Gutsev, G. L.; Khanna, S. N.; Rao, B. K.; Jena, P. *J. Phys. Chem. A* **1999**, *103*, 5812. (b) Gutsev, G. L.; Khanna, S. N.; Rao, B. K.; Jena, P. *Phys. Rev. A* **1999**, *59*, 3681.

(22) Atanasov, M. *Inorg. Chem.* **1999**, *38*, 4942.

(23) Cao, Z.; Wu, W.; Zhang, Q. *J. Mol. Struct. (Theochem)* **1999**, *489*, 165.

(24) Wang, G. J.; Zhou, M. F. *Int. Rev. Phys. Chem.* **2008**, *27*, 1.

(25) Frisch, M. J.; Trucks, G. W.; Schlegel, H. B.; Scuseria, G. E.; Robb, M. A.; Cheeseman, J. R.; Montgomery, J. A., Jr.; Vreven, T.; Kudin, K. N.; Burant, J. C.; Millam, J. M.; Iyengar, S. S.; Tomasi, J.; Barone, V.; Mennucci, B.; Cossi, M.; Scalmani, G.; Rega, N.; Petersson, G. A.; Nakatsuji, H.; Hada, M.; Ehara, M.; Toyota, K.; Fukuda, R.; Hasegawa, J.; Ishida, M.; Nakajima, T.; Honda, Y.; Kitao, O.; Nakai, H.; Klene, M.; Li, X.; Knox, J. E.; Hratchian, H. P.; Cross, J. B.; Adamo, C.; Jaramillo, J.; Gomperts, R.; Stratmann, R. E.; Yazyev, O.; Austin, A. J.; Cammi, R.; Pomelli, C.; Ochterski, J. W.; Ayala, P. Y.; Morokuma, K.; Voth, G. A.; Salvador, P.; Dannenberg, J. J.; Zakrzewski, V. G.; Dapprich, S.; Daniels, A. D.; Strain, M. C.; Farkas, O.; Malick, D. K.; Rabuck, A. D.; Raghavachari, K.; Foresman, J. B.; Ortiz, J. V.; Cui, Q.; Baboul, A. G.; Clifford, S.; Cioslowski, J.; Stefanov, B. B.; Liu, G.; Liashenko, A.; Piskorz, P.; Komaromi, I.; Martin, R. L.; Fox, D. J.; Keith, T.; Al-Laham, M. A.; Peng, C. Y.; Nanayakkara, A.; Challacombe, M.; Gill, P. M. W.; Johnson, B.; Chen, W.; Wong, M. W.; Gonzalez, C.; Pople, J. A. *Gaussian 03, Revision B.05*; Gaussian, Inc.: Pittsburgh, PA, 2003.

(26) Becke, A. D. *Phys. Rev. A* **1988**, *38*, 3098.

(27) Perdew, J. P. *Phys. Rev. B* **1986**, *33*, 8822.

(28) (a) McLean, A. D.; Chandler, G. S. *J. Chem. Phys.* **1980**, *72*, 5639. (b) Krishnan, R.; Binkley, J. S.; Seeger, R.; Pople, J. A. *J. Chem. Phys.* **1980**, *72*, 650.

(29) Zhao, Y. Y.; Gong, Y.; Zhou, M. F. *J. Phys. Chem. A* **2006**, *110*, 10777.

(30) (a) Zhang, L. N.; Zhou, M. F.; Shao, L. M.; Wang, W. N.; Fan, K. N.; Qin, Q. Z. *J. Phys. Chem. A* **2001**, *105*, 6998. (b) Wang, X. F.; Zhou, M. F.; Andrews, L. *J. Phys. Chem. A* **2000**, *104*, 10104. (c) Zhou, M. F.; Liang, B. Y.; Andrews, L. *J. Phys. Chem. A* **1999**, *103*, 2013.

(31) Wang, G. J.; Chen, M. H.; Zhou, M. F. *J. Phys. Chem. A* **2004**, *108*, 11273.

(32) (a) Gong, Y.; Zhou, M. F.; Tian, S. X.; Yang, J. L. *J. Phys. Chem. A* **2007**, *111*, 6127. (b) Gong, Y.; Zhou, M. F. *J. Phys. Chem. A* **2007**, *111*, 8973. (c) Gong, Y.; Ding, C. F.; Zhou, M. F. *J. Phys. Chem. A* **2007**, *111*, 11572. (d) Gong, Y.; Wang, G. J.; Zhou, M. F. *J. Phys. Chem. A* **2008**, *112*, 4936.

(33) Cramer, C. J.; Tolman, W. B.; Theopold, K. H.; Rheingold, A. L. *Proc. Natl. Acad. Sci. U.S.A.* **2003**, *100*, 3635.

(34) Rollason, R. J.; Plane, J. M. C. *Phys. Chem. Chem. Phys.* **2000**, *2*, 2335.

(35) (a) Zhou, M. F.; Citra, A.; Liang, B. Y.; Andrews, L. *J. Phys. Chem. A* **2000**, *104*, 3457. (b) Bare, W. D.; Souter, P. F.; Andrews, L. *J. Phys. Chem. A* **1998**, *102*, 8279.

(36) (a) Chertihin, G. V.; Bare, W. D.; Andrews, L. *J. Chem. Phys.* **1997**, *107*, 2798. (b) Zhou, M. F.; Andrews, L. *J. Chem. Phys.* **1999**, *111*, 4230.

(37) (a) Chertihin, G. V.; Bare, W. D.; Andrews, L. *J. Phys. Chem. A* **1997**, *101*, 5090. (b) Zhou, M. F.; Andrews, L. *J. Phys. Chem. A* **1998**, *102*, 8251.

(38) (a) Chertihin, G. V.; Citra, A.; Andrews, L.; Bauschlicher, C. W., Jr. *J. Phys. Chem. A* **1997**, *101*, 8793. (b) Danset, D.; Alikhani, M. E.; Manceron, L. *J. Phys. Chem. A* **2005**, *109*, 97. (c) Citra, A.; Andrews, L. *J. Phys. Chem. A* **1999**, *103*, 4845. (d) Yang, R.; Gong, Y.; Zhou, H.; Zhou, M. F. *J. Phys. Chem. A* **2007**, *111*, 64. (e) Citra, A.; Andrews, L. *J. Phys. Chem. A* **1999**, *103*, 4182.

(39) Gong, Y.; Zhou, M. F. *J. Phys. Chem. A* **2008**, *112*, DOI: 10.1021/jp805495d.

JP806442Y